Computing the Age-Related Dysfunction of Cardiac Pacemaker

H Zhang[1], JH Liu[2], AV Holden[3]

[1]The University of Manchester, UK
[2]Northeastern University, PR China
[3]The University of Leeds, UK

Abstract

In both human and animal mammals, the pacemaker of the heart, the sinoatrial node (SA node), deteriorates with age. The main features of the aged SA nodes are a slow pacemaking rate and possible SA node-atrium conduction exit block or arrest of SA node pacemaking (i.e., termination of the SA node pacemaker activity). The mechanisms underlying the age-related dysfunction of the heart are unclear. In this study, we developed a detailed computer model of normal and aged SA nodes. Using the model we evaluated the functional roles of age-dependent reduction in SA node i_{Na} current and active cell population in initiation and conduction of pacemaker activity in the aged heart. Simulations have shown that decrease in the SA node i_{Na} or active cell population results in an increase of pacemaking cycle length (equivalent to a decrease of pacemaking rate) and slowing down of SA node-atrium conduction. It also produces the SA node–atrium conduction block in which action potentials originating from the SA node can fail to conduct into the atrium, or termination of the SA node pacemaker activity. When considered together, combined actions have a greater impact on weakening the pacing and driving ability and producing impairment of impulse initiation and conduction that leads to the SA node-atrium conduction exit block. These simulations provide mechanistic insights for understanding the dysfunction of the SA node in aged hearts.

1. Introduction

In human and other mammals, the functions of the pacemaker of the heart, the SA node declines with ageing (1, 2, 5, 8). The main features of the aged SA nodes are a slow pacemaking rate (i.e., increase in CL) and possible SA node-atrium conduction exit block or arrest of SA node pacemaking (i.e., termination of the SA node pacemaker activity) (1, 2, 5). There is experimental evidence for the associations between ageing and changes in the electrophysiological and anatomic properties of the SA node. In humans, it was found that there is about 16% reduction in the active SA node cells in the elderly compared to adults (8). In the rabbit heart, several studies suggested a possible reduction of i_{Na} in aged SA nodes (2, 3, 5). It is unclear whether or not such ageing-dependent changes can account for the deterioration of the SA node with ageing. In this study, we used a biophysically detailed computer model of the SA node and surrounding atrium to evaluate how a reduction of i_{Na} or a decrease in active SA node cell population, or both combined, affects the cardiac pacemaker activity.

2. Methods

The SA node is a complicated tissue with heterogeneities in cell electrical properties and anatomical structures (5). Based on the measured regional differences of ionic current densities and their relations to cell size, we have developed mathematical models of action potentials of the rabbit central and peripheral SA node cells (10-13). These models generated action potentials having the same characteristics as those recorded experimentally (10). In this study, we used the Zhang et al. models to simulate the electrical action potentials of central and peripheral SA node cells.

A 2D model of the intact SA node and surrounding atrium tissue was constructed by incorporating the Zhang et al. single cell models into a 2D coupled ordinary different equation network (13). At each node of the network, electrical action potential is modeled by a set of ordinary differential equations, which can be represented as

$$\frac{dV}{dt} = -\frac{1}{C_m} i_{tot}$$
$$i_{tot} = i_{Na} + i_{Ca,L} + i_{Ca,T} + i_{to} + i_{sus} + i_{K,r} + i_{K,s} + i_f + i_{b,Na} + i_{b,Ca} + i_{b,K} + i_{NaCa} + i_p \quad (1)$$

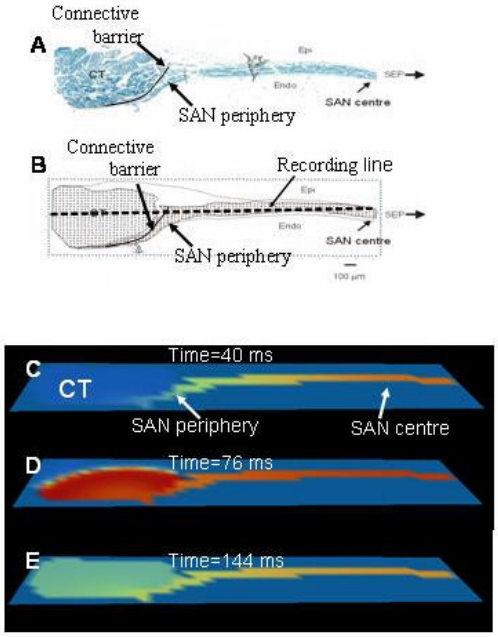

Figure 1. (A) A toluidene blue stained tissue section through the SA and its surrounding atrial muscle of the crista terminalis cut through the leading pacemaker site. (B) A two-dimensional lattice model of the SA node and its surrounding atrium (A). (C-E) Snapshot of initiation and conduction of the pacemaker activity after 40 ms (C), 76 ms (D) and 144 ms (E). Figure modified from (13).

In the equation (1), V is the cell membrane potential (in mV), t the time (in s), C_m the cell membrane capacitance (in μF), i_{tot} the total membrane ionic channel currents (in nA). For details of the equations and parameters please see (10). Heterogeneous electrical properities of the SA node were also considered. For a cell(i,j) in the lattice, where i & j indexe x- and y-coordinate, if cell(i,j) is a SA node cell, then the cell capacitance and ionic current densities are correlated to each other and vary spatially. Across the SA node, we assumed that cells in the centre are small while cells in the periphery are large. Correspondingly C_m (cell capacitance) changed from 20pF in the centre to 65pF in the periphery:

$$C_m^s(i,j) = 20 + \frac{0.9(3.22 - 0.035i)}{3.22\left(1 + 0.8e^{-(1.12-0.035i)/(0.1225)}\right)}(65-20)$$

$$g^s(i,j) = \frac{\left(65 - C_m^s(i,j)\right)g_c + \left(C_m^s(i,j) - 20\right)g_p}{65-20} \qquad (2)$$

If cell(i,j) is an atrial cell, then the cell electrical properties were assume to be identical and is modelled by the Earm-Hilgemann-Noble model (7).

Electrotonic interaction between cardiac cells was modelled by a gap junctional conductance g(i,j). Each node in the lattice was electrically coupled to its four nearest neighbouring nodes. Thus for a cell(i,j), its membrane potential is governed by:

$$C_m^a(i,j)\frac{dV^a(i,j)}{dt} = -i_{tot}^a(i,j) + g^a(i,j+1)(V^a(i,j+1) - V^a(i,j)) + g^a(i,j-1)(V^a(i,j-1) - V^a(i,j)) + g^a(i+1,j)(V^a(i+1,j) - V^a(i,j)) + g^a(i-1,j)(V^a(i-1,j) - V^a(i,j)) \qquad (3)$$

At boundary, If *cell(i+l, j+m)* is non-cardiac cell or empty, *l* and *m* index the neighbourhood of *cell (i,j)* and *(l,m)∈[-1,+1]*, then:

$$g(i+l,j+m)(V(i+l,j+m) - V(i,j)) = 0$$

The junctional conductance was set to 25 nS for SA node-SA node cell or SA node-atrial cell, and 175 nS for atrial-atrial cells. In the equations, *s* denotes the SA node, *a* denotes the atrium.

In order to classify the spatial structure of the model, a slice of SA node and atrium tissue was cut from the middle of the rabbit SA node perpendicularly to the crista terminalis. The tissue was then discretised by a spatial resolution of 35 μm to generate a two-dimensional discrete lattice with 91×28 nodes (Figure 1). Using detailed information from molecular mapping, we classified each node in the lattice as either a SA node cell or an atrial cell.

The model was numerically solved by an explicit Euler method with a time step of 0.1 ms. The chosen time step are sufficiently small for a stable and accurate solution. In simulations, action potentials were recorded for cells on the recording line as shown in Figure 1 (cells spatially distributed from centre towards periphery of SA node and atrium) and were plotted to display initiation and propagation of action potentials (space: vertically; time: horizontally). Cycle length (CL) was measured as the time interval between two successive action potentials recorded from the SA node (*cell(90,15)*).

3. Results

The effects of age-dependent i_{Na} reduction on initiation and conduction of the pacemaker activity of the SA node were investigated by simulations performed under control and i_{Na} removal from the SA node conditions. These results are shown in Figure 2, which represented the space-time plot of action potentials of cells on the recording line under control (Figure 2A) and SA node i_{Na}

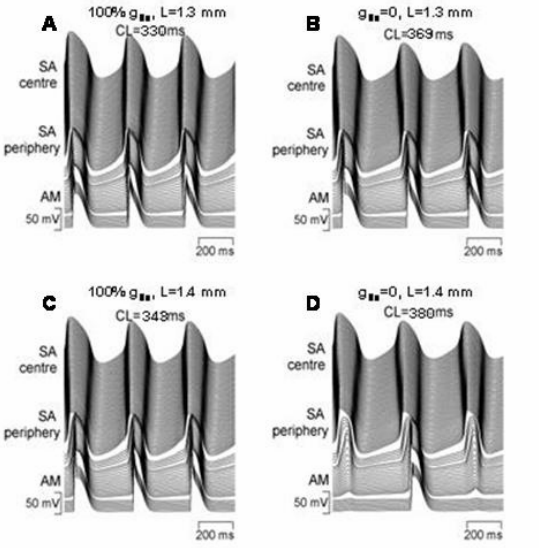

Figure 2. (A,B) Action potentials recorded from cells along the recording line with L=1.3 mm under control (A) and 100% i_{Na} reduction (B). (C,D) Simulations under conditions similar to (A, B) but with L=1.4 mm.

removal by 100% (Figure 2B). Deduction of SA node i_{Na} current slowed down pacemaker activity - the measured CL increased from 330 ms under control to 369 ms when i_{Na} was removed.

Effects of SA node i_{Na} removal on the SA node pacemaker activity are dependent on the extent of electrotonic coupling between the SA node and atrium. Figure 2C and 2D show similar simulations but with increased physical contact area (L= 1.4 mm) between the SA node and atrium. This resulted in a stronger electrotonic interaction between the two tissues and augmented the role of SA node i_{Na} reduction in slowing down the SA node to pace and drive the atrium. Under control condition, the measured CL was 343 ms. But when SA node i_{Na} was removed by 100%, the SA node continued oscillating at a slow rate (the measured CL was 380 ms), failed to drive atrium from beat to beat. SA node driving alternans occurred: a beat that drove atrium was followed by a beat that failed to drive atrium. This alternant driving phenomenon is similar to the SA node conduction exist block observed in aged hearts or hearts with the sick sinus syndrome (SSS) (1-2, 4-6, 9).

i_{Na} removal also slowed down the conduction of the pacemaker activity within the SA node and atrial tissue. Figure 3 plotted the measured sinoatrial node conduction time (SACT) under control and various i_{Na} removal conditions. Reduction of SA node i_{Na} increased the SACT monotonically. By 50% and 95% of SA node i_{Na} removal, the SACT was increased by 15 ms and 35 ms respectively

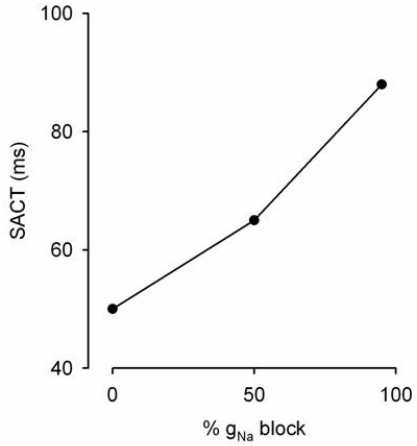

Figure 3. The computed SACT with different percentages of SA node i_{Na} removal.

compared to control condition (0% deduction). The computed SACT with i_{Na} removal shows similar increase pattern as observed in the aged rabbit SA node (2).

A series of simulations was also performed to investigate the possible actions of age-dependent reduction in the active SA node cell population on the pacemaker activity. In simulations, CL was measured for 1%, 5%, 10% and 15% reduction of the active SA node cells. Reduction of active SA node cells slowed down the pacemaking rate, which was demonstrated by an increase in the measured CL. By 1%, 5% and 10% cell reduction, the measured CL was 332 ms, 337 ms and 347 ms respectively, an increase of 2, 7 and 17 ms from 330 ms when no dead cells were present. By 15% reduction in the active SA node cells, the SA node terminated its pacemaker activity. A 15% reduction in the active cell population is close to the experimentally reported 16% cell death in the elderly patients in humans (38). A 10% reduction in active SA node cell population had negligible effect on the measured SACT (4 ms increase compared to the control condition).

Combined actions of cell death and reduction of SA i_{Na} current density were also studied. Figure 4 shows the initiation and conduction of the pacemaker activity for 10% cell death (4A), 10% cell death together with 100% (4B) of SA node i_{Na} removal. In all cases, combined actions of cell death and i_{Na} removal had greater impacts on slowing down the pacemaking rate compared to the actions of cell death only or actions of i_{Na} removal only. The measured CL for 100% removal i_{Na} from the SA node was 382 ms, an increase of 54 ms from 330 ms under control condition.

Figure 4C and D represented results obtained with L=1.4 mm, together with a 10% loss of cell population

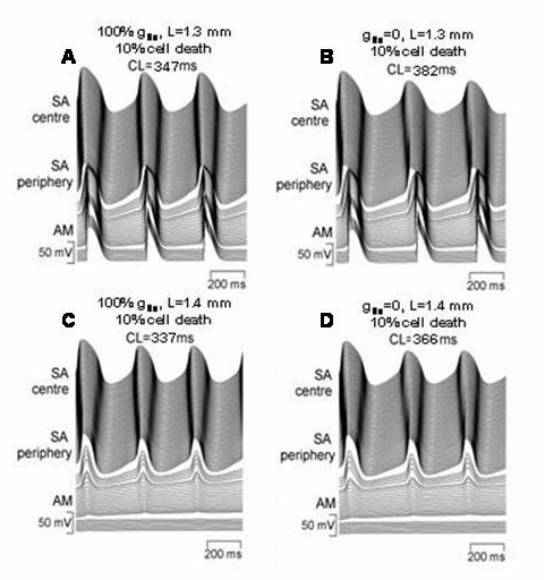

Figure 4. (A,B) Action potentials recorded from cells along the recording line with L=1.3 mm and various levels of reductions in i_{Na} and active cell populations in the SA node. A: 10% dead SA node cell population only. B: 100% i_{Na} reduction and 10% dead SA node cell population. (C,D) are stimulations under conditions similar to A and B respectively but with L=1.4 mm.

and i_{Na} removed by 0 and 100% respectively. In all cases, the SA node paced stably, but failed to drive atrium.

4. Discussion and conclusions

In this study, we used a 2D anatomical model of the intact SA node and atrium to evaluate the functional roles of age-related changes in the properties of the SA node (i_{Na} reduction and cell death) on initiation and conduction of the pacemaker activity. We found that reduction of SA node and/or active SA node cell population slows down the pacemaking rate and compromises the conduction of the pacemaker activity by increasing the sinoatrial node atrium conduction time; it can also lead to SA node exit block or sinus arrest. These behaviours are main features of aged hearts or the hearts with SSS (2, 5, 14-16, 36-37). We concluded that the age-dependent deterioration can be accounted for by the age-related reduction in the SA node i_{Na} and active cell population. This study provides further insights into understanding the mechanisms underlying dysfunctions of the SA node in SSS and aged hearts.

Acknowledgements

This work was supported by project grants from BHF (PG/03/140/16236) and BBSRC (BBS/B1678X) and EU-Network of Excellence (BioSim) (005137).

References

[1] Alings, A. M. & Bouman, L. N. Electrophysiology of the ageing rabbit and cat sinoatrial node - comparative study. Eur Heart J 1993; 14: 1278-1288.

[2] Alings, A. M, Abbas, R.F, Bouman, L.N. Age-related changes in structure and relative collagen content of the human and feline sinoatrial node. A comparative study. Eur Heart J 1995; 16: 1655-1667.

[3] Baruscotti, M., DiFrancesco, D. & Robinson, R. B. A TTX-sensitive inward sodium current contributes to spontaneous activity in newborn rabbit sino-atrial node cells. J Physiol 1996; 492: 21-30.

[4] Benson, D. W., Wang, D. W., Dyment, M., Knilans, T. K., Fish, F. A., Strieper, M. J., Rhodes, T. H. & George, A. L. Jr. Congenital sick sinus syndrome caused by recessive mutations in the cardiac sodium channel gene (SCN5A). J Clin Invest 2003; 112: 1019-1028.

[5] Boyett, M. R., Honjo, H. & Kodama, I. The sinoatrial node, a heterogeneous pacemaker structure. Cardiovasc Res 2000; 47**:** 658-687.

[6] Gregorators, G. Sick sinus syndrome. Circulation 2003; 108: e143-144.

[7] Noble, D. Oxsoft manual version 4.8. Oxford . 1990.

[8] Shiraishi, I., Takamatsi, T., Minamikawa, T., Onouchi, Z. & Fujita, S. Quantitative histological analysis of the human sinoatrial node during growth and aging. Circulation 1992; 85**:** 2176-2184.

[9] Veldkamp, M. W., Wilders, R., Baartscheer, A., Zegers, J. G., Bezzina, C. R. & Wilde, A. A. Contribution of sodium channel mutations to bradycardia and sinus node dysfunction in LQT3 families. Circ Res 2003; 92: 976-983.

[10] Zhang, H., Holden, A. V. and Boyett, M. R. The gradient model vs the MOSAIC model. Circulation 2001; 103: 584-588.

[11] Zhang, H., Holden, A. V., Kodama, I., Honjo, H., Lei, M., Varghese, T. & Boyett, M. R. Mathematical models of action potentials in the periphery and centre of rabbit sinoatrial node. Am. J. Physiol. Heart. Circ. Physiol 2000;. 279 (1): H397-H421.

[12] Zhang, H., Dobrzynski, H., Holden A. V., Boyett, M. R. Heterogeneous sinoatrial node of rabbit heart-molecular and electrical mapping and biophysical reconstruction. LNCS 2003; 2674: 132-140.

[13] Zhang, H., Zhao, Y., Lei, M., Dobrzynski, H., Liu, J.H., Holden, A.V. and Boyett, M.R. Computational evaluation of the role of Na+ current, i_{Na}, and cell death in cardiac pacemaking and driving. Am J Physiol (Heart Circ & Physiol) 2006; In press.

Address for correspondence

Dr. Henggui Zhang
Sackville Street Building
School of Physics & Astronomy
Manchester, M60 1QD, UK
E-mail: Henggui.zhang@manchester.ac.uk